Title
SEQUENCE OF PHASE FORMATION IN NB/AL MULTI-LAYERED SAMPLES

Author
Morris, J.W.

Publication Date
1988-05-01

LBL-25466

c.2

Center for Advanced Materials

CAM

Submitted to Journal Applied Physics

Sequence of Phase Formation in Nb/Al Multi-Layered Samples

Y. Im and J.W. Morris, Jr.

May 1988

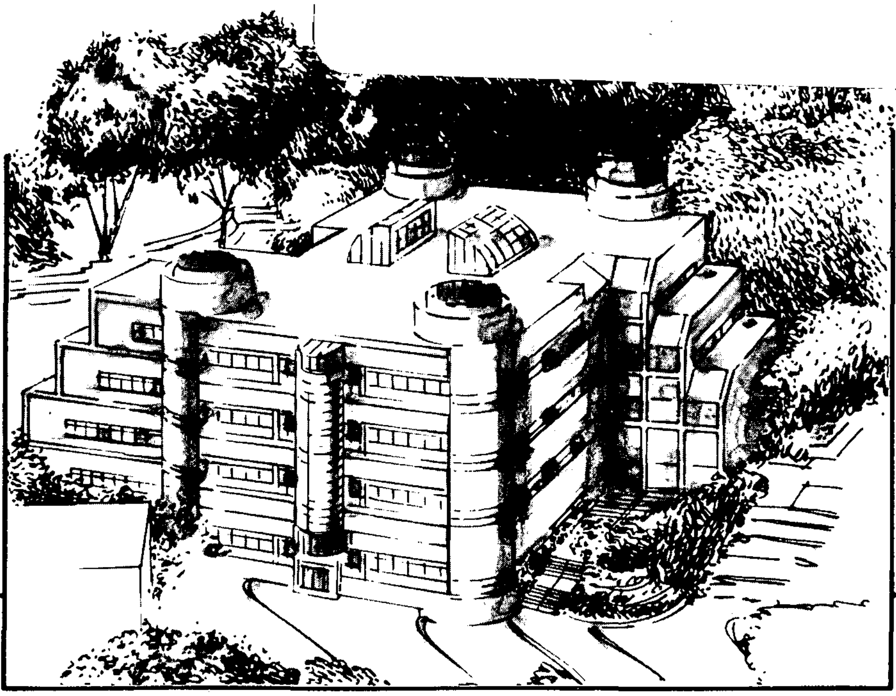

Materials and Chemical Sciences Division

Lawrence Berkeley Laboratory • University of California

ONE CYCLOTRON ROAD, BERKELEY, CA 94720 • (415) 486-4755

Prepared for the U.S. Department of Energy under Contract DE-AC03-76SF00098

LBL-25466
c.2

DISCLAIMER

LBL 25466

Sequence of Phase Formation in Nb/Al Multi-Layered Samples

Yoonsoon Im and J. W. Morris, Jr.

Center for Advanced Materials
Materials and Chemical Sciences Division
Lawrence Berkeley Laboratory
University of California

and

Department of Materials Science and Mineral Engineering
University of California at Berkeley
Berkeley, California 94720

May 1988

This work is jointly supported by the Director, Office of Energy Research, Office of Fusion Energy, Development and Technology Divison of the U. S. Department of Energy under Contract No. DE-AC03-76SF00098

Sequence of Phase Formation in Nb/Al Multi-Layered Samples

Yoonsoon Im and J. W. Morris, Jr.

Center for Advanced Materials, Lawrence Berkeley Laboratory
Dept. of Materials Science and Engineering
University of California, Berkeley

A series of Nb/Al multi-layered samples made by a sputter-deposition or a cold-rolling technique was used to simulate reactions in powder metallurgy processed Nb/Al superconducting wires. The sequence of phase formation observed in the Nb/Al multi-layered samples was explained using knowledge about the crystal structure of each compound. Three different controlling mechanisms were proposed: the activation energy for nucleation, the energy barrier associated with short range order, and the diffusion barrier by the previously formed phase layer.

Introduction

Reactions at the Nb/Al interface are of particular interest because one of the phases formed is the superconducting Nb_3Al. Nb_3Al is a good candidate for a high field superconductor that could replace Nb_3Sn or NbTi currently in commercial use[1][2].

Nb_3Al formation in powder metallurgy (P/M) processed Nb/Al superconducting wires has been widely studied[2]-[9]. In the P/M approach, elemental Nb and Al powders are plastically deformed into thin ribbon-like filaments between which a Nb/Al interface is created. The microstructure of the P/M processed wires is so inhomogeneous that it is very difficult to study reactions at the Nb/Al interface. Bormann et. al. studied reactions at Nb/Al interfaces using sputter-deposited Nb/Al multi-layered samples[10]. Since their work was solely based on an X-ray diffraction technique, only indirect microstructural information was obtained.

Recently, the authors made samples similar to those of Bormann's in order to investigate the interfacial reactions using transmission electron microscopy[11]. Samples with both 1000Å Nb/ 270Å Al and 300Å Nb/ 80Å Al multi-layers were reacted to form $NbAl_3$ with some remaining Nb after a 600°C/100hrs heat treatment. The $NbAl_3$ phase reacted with remaining Nb to form the superconducting Nb_3Al phase when the samples were further heat treated at 900°C for 20min. $NbAl_3$ formed when a sample with 630 Å Al layers was heat treated at 600°C. The $NbAl_3$ phase and remaining Nb reacted to form a $Nb_3Al/Nb_2Al/Nb_3Al$ layer configuration after a heat treatment at 900°C for 20min. In the case of a Nb/Al diffusion-couple sample with a 0.5mm Al layer, only $NbAl_3$ was observed regardless of heat treatment conditions. This sequential phase formation at Nb/Al interfaces has not yet been explained.

Sequential phase formation has also been frequently observed in other thin film systems such as Ni/Si[12], Co/Si[13], Pd/Al[14], Pt/Al[15], Au/In[16] and Cu/Al[17][18]. Usually the compounds are formed one by one in sequence; the appearance of a new phase being generally accompanied by the disappearance of the previously formed compounds. There have been efforts to predict the sequence of phase formation in thin films using equilibrium phase diagrams[19]-[21]. Kirkadly argued that a condition of (near-) equilibrium must exist at phase interfaces[22]. Eifert suggested that the interface compositions were essentially time constant although not those predicted by the equilibrium tie-lines[23].

However, formation of amorphous phases during solid state reactions has been observed and indicates that kinetics is responsible for the early state of reactions[24]-[26]. d'Heurle and Gas discussed reaction mechanisms in Ni/Si and Co/Si thin films[27]. They divided the reactions into three categories: diffusion-controlled, nucleation-controlled and reaction-rate-controlled. Gösele and Tu[28] have demonstrated that the competition between interface-controlled and diffusion-controlled phenomena has specific effects on the sequence of phase formation, but their model failed to predict which compound was kinetically favorable in the competition in nucleation between compounds. Most of the work on thin film reactions concerns the controlling mechanisms that are related to the growth of *already* nucleated phases rather than prediction of a particular phase formation. Meng et al. suggested that differences in the relative ease of nucleation and differences in diffusivities are factors which determine the formation of the particular phases at Ni/Ti and Ni/Zr interface[29].

Experimental procedure

Nb/Al multi-layered samples with various Nb/Al layer configurations were made in an attempt to determine the reaction mechanisms at the Nb/Al interface. Two sets of samples were made by sputtering Nb and Al alternatively on Nb or Si wafer substrates, with the thickness of the multi-layers being 300Å Nb/ 80Å Al and 1000Å Nb/ 270Å Al respectively (Fig. 1). Samples with thicker multi-layers were prepared by a cold-rolling technique. Several Nb plates were polished, cleaned and coated with Al in a vacuum chamber. The stack of Al-coated Nb plates were then put into a 1/4" diameter Al tube and cold-rolled into a multi-layered sample. It was not possible to control Al layer thickness precisely in this way, but it was a straightforward method of producing Nb/Al layers with Al layers of submicron to micron thickness.

The samples were heat treated at temperatures ranging between 300°C and 1100°C for various lengths of time in a vacuum-encapsulated quartz tube backfilled with Ar gas. A variety of techniques was used for characterization: X-ray diffraction, optical microscopy, scanning electron microscopy and transmission electron microscopy with convergent beam microdiffraction and EDX capabilities. Cross-sectional T.E.M. specimens of multi-layered samples were made by dimpling followed by ion milling.

Results

For heat treatments below 650°C, the tetragonal $NbAl_3$ phase was found to form regardless of holding time at temperature and Nb/Al layer configuration. The $NbAl_3$ phase formed after a short heat treatment at a temperature as low as 300°C. The composition of $NbAl_3$ was measured by EDX to be about 75 atom% Al. Nb layers remaining after reactions contained no measurable Al in solid solution.

For heat treatments above 700°C, however, the reactions were affected by the Al layer thickness provided there was a sufficient Nb supply. When the Al layers were thinner than 300Å, all the Al was consumed to form the superconducting Nb_3Al phase. Some samples were reacted at 600°C for 100 hrs prior to a higher temperature heat treatment above 700°C. The $NbAl_3$ phase that formed during the 600°C heat treatment reacted with remaining Nb to form Nb_3Al. A Nb-Al solid solution and Nb_2Al as well as Nb_3Al were reported to form in the sample with 1000Å Nb/300Å Al layers by Bormann et al. but were not seen in this work. Reactions at the Nb/Al interface with thicker Al layers (>300Å) were studied using the cold-rolled samples. The microstructure of a sample with 630Å thick Al layers heat treated at 900°C/20min showed a $Nb_3Al/Nb_2Al/Nb_3Al$ layer configuration. For samples with very thick Al layers, only $NbAl_3$ was found to grow regardless of heat treatment conditions as long as both the Nb and Al layers remained. Nb-Al solid solution was not found in any of the cases. The results of the reactions are summarized in table 1.

Discussion

The reactions at the Nb/Al interface cannot be explained from the Nb/Al binary phase diagram[30]. The Nb/Al equilibrium phase diagram, shown in Fig. 2, indicates that Nb-Al solid solution, Nb_3Al, Nb_2Al and $NbAl_3$ are expected to be thermodynamically stable over a large temperature range. In the case of Nb/Al multi-layered samples, however, not all of the phases predicted by the equilibrium phase diagram were observed simultaneously; phase formation occurred in sequence.

An effort was made to explain the sequential phase formations in the Nb/Al thin films using knowledge about the crystal structure of each compound. $NbAl_3$ has the DO_{22} tetragonal structure and can easily form by substitutionally replacing 2 Al atoms with Nb atoms in 2 fcc Al unit cells. Fig. 3a illustrates the structural similarity between $NbAl_3$ and Al. The superconducting Nb_3Al phase has the A15 type cubic structure, with 6 Nb atoms being interstitially placed at the distorted tetrahedral sites in the bcc Al sub-structure (Fig. 3b). The Nb_2Al phase has the tetragonal sigma structure, with 30 atoms per unit cell as shown in Fig. 3c.

Using knowledge about the crystal structures of the compound phases, three reaction mechanisms are proposed to explain the reactions at the Nb/Al interface.

The Activation energy for nucleation:

For heat treatments below 650°C, $NbAl_3$ formed regardless of holding time at temperature and Nb/Al layer configuration. We believe that Nb_3Al and Nb_2Al could not overcome the activation energy for nucleation at these low temperatures. According to classical nucleation theory, the competition between the volume free energy ΔG and the surface energy σ gives rise to the activation energy for nucleation which is proportional to $\sigma^3/\Delta G^2$. Since the structure of $NbAl_3$ is similar to that of Al, the interfacial free energy between Al and $NbAl_3$ is thought to be very low. Thus the nucleation of $NbAl_3$ at the Nb/Al interface is kinetically favored, and $NbAl_3$ can nucleate at relatively low temperatures (<650°C) regardless of Al layer thickness as illustrated in Fig. 4.

The energy barrier associated with short range order:

At reaction temperatures above 700°C, reactions were affected by the Al layer thickness. $NbAl_3$ continued to grow as long as both Nb and Al layers remained. Nb_3Al formed in samples with Al layers thinner than 300Å, while Nb_2Al did not form. We propose that the reactions at higher temperatures are governed by the energy barrier associated with short range order to form an ordered state.

Formation of the $NbAl_3$ phase requires less rearrangement of atoms than that of Nb_3Al. The largest rearrangement of Nb and Al atoms, however, is required to form the Nb_2Al phase whose unit cell is composed of 30 atoms. Therefore, the energy barrier associated with short range order is smallest for $NbAl_3$ formation and largest for Nb_2Al formation. Consequently, the kinetically favorable $NbAl_3$ phase will grow continuously as long as both Nb and Al layers remain. When all the Al is consumed to form the $NbAl_3$ phase, the next favorable Nb_3Al will start to form at the $Nb/NbAl_3$ interface (Fig. 5). If the reacted $NbAl_3$ layer is sufficiently thin, all the $NbAl_3$ phase will react with remaining Nb to form the superconducting Nb_3Al phase as observed in the sputter-deposited samples.

The diffusion barrier controlled mechanism:

When the Al layers were between 300Å and 1µm, Nb_2Al formed between two Nb_3Al phase layers at reaction temperatures above 700°C as described in table 1. The average grain size of Nb_2Al was much smaller than that of the Nb_3Al phase. The thickness of the Nb_3Al layers was about 700Å-800Å regardless of the initial Al layer thickness. Fig. 7 shows that Nb_2Al started to form between Nb_3Al and $NbAl_3$ layers. If Nb_2Al formed by consuming Nb_3Al and $NbAl_3$, then the thickness of the resulting Nb_3Al layers would be dependent on the thickness of Nb_2Al between the Nb_3Al layers. Therefore we concluded that Nb_3Al phase did not dissolve after it formed.

Formation of the Nb_2Al phase can be explained by a diffusion-barrier controlled mechanism. Nb diffusion through a Nb_3Al layer is expected to be much slower than through a $NbAl_3$ layer. When Nb_3Al grains grow to form a continuous layer, further diffusion is allowed only through the Nb_3Al grain boundaries. An insufficient Nb supply causes the formation of the Nb-depleted Nb_2Al phase to become kinetically favorable, resulting in the $Nb_3Al/Nb_2Al/Nb_3Al$ layer configuration (Fig. 6).

This mechanism can explain why the Nb_3Al layers do not grow thicker than a certain thickness. Since diffusion is very limited through the Nb_3Al phase, Nb_3Al grains will grow faster laterally along the $Nb/NbAl_3$ boundaries than to the perpendicular direction. When they grow large enough to form a continuous layer, grain growth stops and the resulting Nb_3Al grains tend to have elongated shapes. However, we do not understand why Nb_3Al does not react with $NbAl_3$ to form the Nb_2Al phase as expected from the Nb/Al equilibrium phase diagram. More work on multi-layered samples is planned to better understand the Nb_2Al phase formation.

The proposed reaction mechanisms are consistent with observations in powder metallurgy processed Nb/Al superconducting wires:

1] $NbAl_3$ forms below 650°C while Nb_3Al and Nb_2Al form above 700°C.

2] The $Nb_3Al/Nb_2Al/Nb_3Al$ configuration is observed.

3] Nb-Al solid solution is not observed.

4] A high reduction ratio (ie. thinner Al layers) yields more Nb_3Al.

Summary

The reactions at Nb/Al interfaces were studied using multi-layered samples made by a sputter-deposition or a cold-rolling technique. Nb/Al layers of various thickness and distribution were used to simulate the reactions in powder metallurgy processed Nb/Al superconducting wires.

It was found that phase formation occurred in sequence. Only $NbAl_3$ formed below 650°C regardless of Nb/Al layer configuration. Above 700°C, reactions were affected by the Al layer thickness. $NbAl_3$ continued to grow as long as Nb and Al layers remained. Nb_3Al formed by consuming $NbAl_3$ and Nb along the $Nb/NbAl_3$ interface. The Nb_3Al formation stopped when it formed a continuous layer. Nb diffused along the Nb_3Al grain boundaries to react with the remaining $NbAl_3$ phase to form the Nb-depleted Nb_2Al.

Three different controlling mechanisms were proposed to explain the sequence of phase formation in Nb/Al multi-layered samples using knowledge about the crystal structure of each compound. $NbAl_3$ formation below 650°C was explained by the activation energy for nucleation. Nb_3Al formation above 700°C was explained by the energy barrier associated with short range order. And the formation of the Nb_2Al phase was explained by the diffusion barrier of the previously formed Nb_3Al layer. Formation of the $Nb_3Al/Nb_2Al/Nb_3Al$ layer configuration was interpreted using the proposed mechanisms. The proposed reaction mechanisms were consistent with observations in P/M processed wires.

Acknowledgement

We are thankful of Dr. J. B. Kortright of the Center for X-ray Optics, Lawrence Berkeley Laboratory for preparing sputter-deposited multi-layered samples. This work was supported by the Director, Office of Energy Resources, Office of Development and Technology, Magnetic Systems Division, U.S. Department of Energy, under contract # *DE-AC03-76SF00098.*

References

1. S. Foner, S. Pourrahimi, C. Thieme, J. Otubo, H. Zhang, T. Orlando, A. Zieba, A. Zaleski, S. Sekine, W. McDonald, R. Roberge, and H. LeHuy
Adv. Cryg. Eng. Mat., Vol. **30** p805 (1984)

2. P. Johnson
M.S. Thesis Dept. Mat. Sci. & Eng. University of California, Berkeley (1987)

3. R. Flükiger, R. Akihama, S. Foner, E. McNiff, Jr., and B. Schwartz
Adv. Cryg. Eng. Mat., Vol. **26** p337 (1980)

4. J. Hong, I. Wu, J. Holthuis, M. Hong, and J. W. Morris, Jr
Presented at the International Cryogenic Materials Conference, San Diego (1981)

5. W. King, C. Thieme and S. Foner
IEEE Trans. Mag., Vol. Mag-**21** No. 2 p815 (1985)

6. P. Johnson, Y. Im, T. McKnelly and J. W. Morris, Jr.
IEEE Trans. Mag., Vol. Mag-**23** No .2, p1432 (1987)

7. R. Akihama, R. Murphy, and S. Foner
Appl. Phys. Lett., **37** (12), p1107 (1980)

8. I. Wu
Ph D. Thesis, Dept. Mat. Sci. & Eng. University of California, Berkeley (1984)

9. S.Pourrahimi, C. Thieme, S. Foner, and R. Murphy
Appl. Phys. Lett., **43** (11) p1070 (1983)

10. R. Bormann, H. Krebs, and A. Kent
Adv. Cryg. Eng. Mat., **32** p1041 (1986)

11. Y. Im, P. Johnson, L. McKnelly, Jr., and J. W. Morris, Jr.
J. Less-Common Metals, **139** p87 (1988)

12. L. R. Zheng, L. S. Hung, and J. W. Mayer
J. Vac. Soc. Tech., **A 1** (2) April-June p758 (1983)

13. A. E. Morgan, E. K. Broadbent, M. Delfino, B. Coulman and D.K. Sadana
Submitted to J. electrochem. Soc.

14. E. G. Colgan
J. Appl. Phys., **62** (6) p2269 (1987)

15. E. G. Colgan

J. Appl. Phys., **62** (4) p1224 (1987)

16. J. P. Goral and L. Eyring
J. Less-Common Metals, **116** p63 (1986)

17. H. T. G. Hentzell, R. D. Thomson, and K. N. Tu
J. Appl. Phys., **54** (12) p6923 (1983)

18. H. T. G. Hentzell, and K. N. Tu
J. Appl. Phys., **54** (12) p6929 (1983)

19. R. M. Walser and R. W. Bene
App. Phys. Lett., Vol. **28** No 10 p624 (1976)

20. Maria Roney
App. Phys. Lett., **42** (7) p577 (1983)

21. B. Y. Tsaur, S. S. Lau, J. W. Mayer, and M. A. Nicolet
App. Phys. Lett., **38** (11) p922 (1981)

22. J. S. Kirkadly
Can. J. Phys., Vol. **36** p917 (1958)

23. J. R. Eifert, D. A. Chatfield, G. W. Powell and J. W. Spretnak
Trans. TMS-AIME, Vol. **242** p66 (1968)

24. R. B. Schwarz and W. L. Johnson
Phys. Rev. Lett., **51** p415 (1981)

25. S. Herd, K. N. Tu and K. Y. Ahn
App. Phys. Lett., **42** p597 (1983)

26. W. L. johnson
Prog. Mat. Sci., **30** p81 (1986)

27. F. M. d'Heurle and P. Gas
J. Mat. Res., 1 (1) Jan/Feb p205 (1986)

28. U. Gösele and K. N. Tu
J. Appl. Phys., **53** (4) p3252 (1982)

29. W. J. Meng, B. Fultz, E. Ma, and W. L. johnson
App. Phys. Lett., **51** (9) p661 (1987)

30. Bulletin of Alloy Phase Diagrams
Vol. **2** No. 1 p75 (1981)

Figure Captions

Fig. 1: T.E.M. micrograph of sputter-deposited Nb/Al multi-layered samples (transverse view) Dark thicker layers are Nb and light thinner layers are Al.
a) 20 pairs of 300Å Nb/ 80Å Al layers were deposited on a Nb substrate.
b) 10 pairs of 1000Å Nb/ 270Å Al layers were deposited on a Nb substrate.

Fig. 2: The equilibrium Nb/Al binary phase diagram indicates that not only Nb_3Al but also Nb_2Al, $NbAl_3$ and Nb-Al solid solution are stable over a large temperature range.

Fig. 3: Crystal structures of compound phases in Nb/Al system
a) $NbAl_3$ has the DO_{22} tetragonal structure which is similar to 2 fcc unit cells.
b) Nb_3Al has the A15 type cubic structure.
c) Nb_2Al has the sigma type tetragonal structure with 30 atoms in a unit cell.

Fig. 4: Since the nucleation of $NbAl_3$ at the Nb/Al interface is kinetically favored, $NbAl_3$ will nucleate at relatively low temperatures (< 650°C) regardless of Al layer thickness.

Fig. 5: The kinetically favorable $NbAl_3$ will grow continuously as long as both Nb and Al remain, and the next favorable Nb_3Al will start to form at the Nb/$NbAl_3$ interface when all the Al is consumed to form $NbAl_3$.

Fig. 6: When Nb_3Al grows to form a continuous layer at the Nb/$NbAl_3$ interface, further Nb diffusion is allowed only through Nb_3Al grain boundaries. An insufficient Nb supply causes the formation of the Nb-depleted Nb_2Al phase resulting in the $Nb_3Al/Nb_2Al/Nb_3Al$ layer configuration.

Fig. 7: T.E.M. micrograph of a cold-rolled Nb/Al multi-layered sample heat treated at 900°C for 10 min (cross sectional view)
Nb_3Al formed a continuous layer and Nb_2Al started to grow at the Nb/Nb_3Al interface. Some remaining $NbAl_3$ is seen in the middle of the reacted region.

Table 1 Sequential phase formation observed in Nb/Al multi-layered samples
Reactions were affected by heat treatment temperature and Al layer thickness.
* $Nb_3Al/Nb_2Al/Nb_3Al$ layer configuration

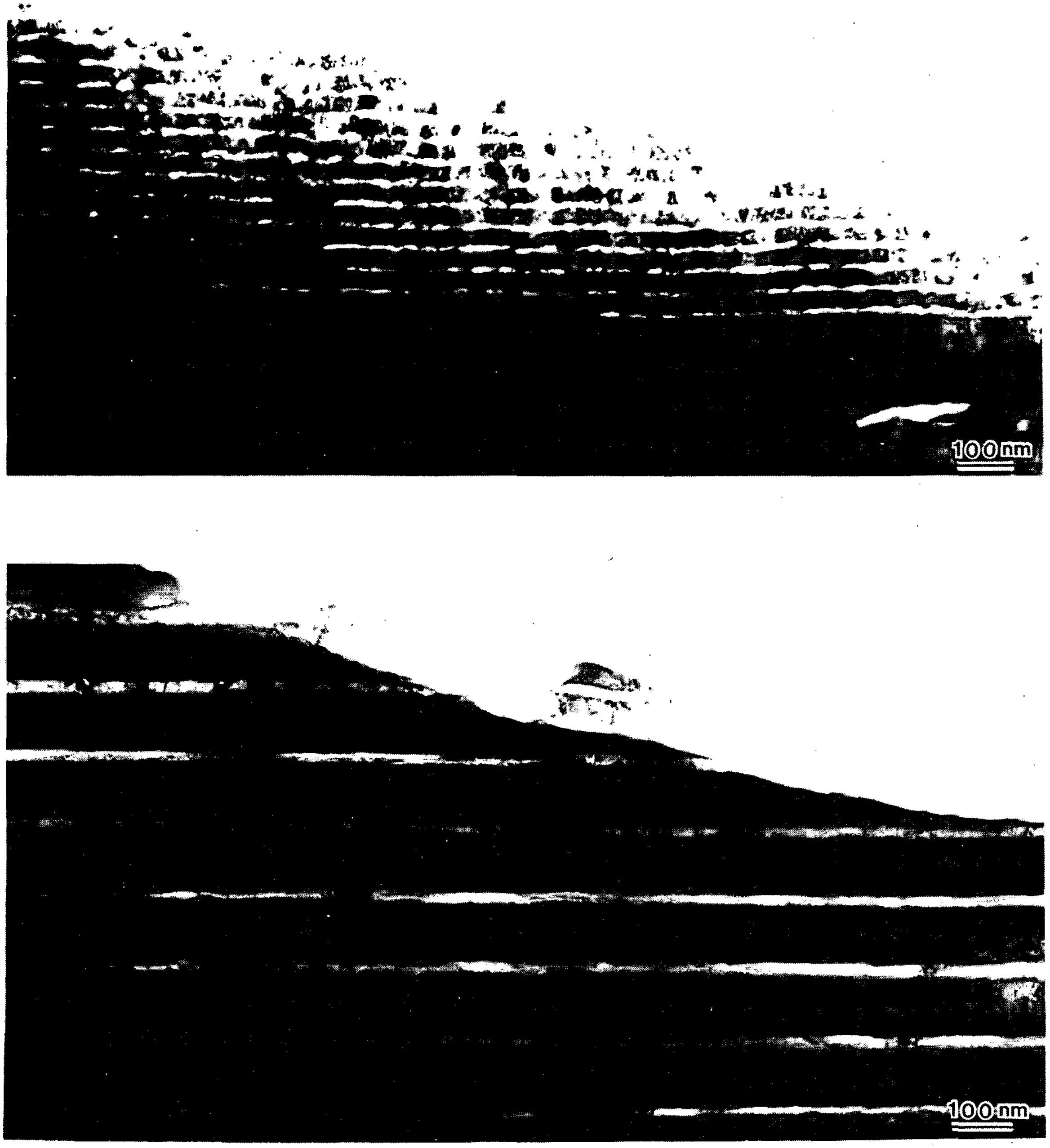

XBB 872-1281

Figure 1

Figure Captions

Fig. 1: T.E.M. micrograph of sputter-deposited Nb/Al multi-layered samples (transverse view) Dark thicker layers are Nb and light thinner layers are Al.
a) 20 pairs of 300Å Nb/ 80Å Al layers were deposited on a Nb substrate.
b) 10 pairs of 1000Å Nb/ 270Å Al layers were deposited on a Nb substrate.

Fig. 2: The equilibrium Nb/Al binary phase diagram indicates that not only Nb_3Al but also Nb_2Al, $NbAl_3$ and Nb-Al solid solution are stable over a large temperature range.

Fig. 3: Crystal structures of compound phases in Nb/Al system
a) $NbAl_3$ has the DO_{22} tetragonal structure which is similar to 2 fcc unit cells.
b) Nb_3Al has the A15 type cubic structure.
c) Nb_2Al has the sigma type tetragonal structure with 30 atoms in a unit cell.

Fig. 4: Since the nucleation of $NbAl_3$ at the Nb/Al interface is kinetically favored, $NbAl_3$ will nucleate at relatively low temperatures (< 650°C) regardless of Al layer thickness.

Fig. 5: The kinetically favorable $NbAl_3$ will grow continuously as long as both Nb and Al remain, and the next favorable Nb_3Al will start to form at the $Nb/NbAl_3$ interface when all the Al is consumed to form $NbAl_3$.

Fig. 6: When Nb_3Al grows to form a continuous layer at the $Nb/NbAl_3$ interface, further Nb diffusion is allowed only through Nb_3Al grain boundaries. An insufficient Nb supply causes the formation of the Nb-depleted Nb_2Al phase resulting in the $Nb_3Al/Nb_2Al/Nb_3Al$ layer configuration.

Fig. 7: T.E.M. micrograph of a cold-rolled Nb/Al multi-layered sample heat treated at 900°C for 10 min (cross sectional view)
Nb_3Al formed a continuous layer and Nb_2Al started to grow at the Nb/Nb_3Al interface. Some remaining $NbAl_3$ is seen in the middle of the reacted region.

Table 1 Sequential phase formation observed in Nb/Al multi-layered samples
Reactions were affected by heat treatment temperature and Al layer thickness.
* $Nb_3Al/Nb_2Al/Nb_3Al$ layer configuration

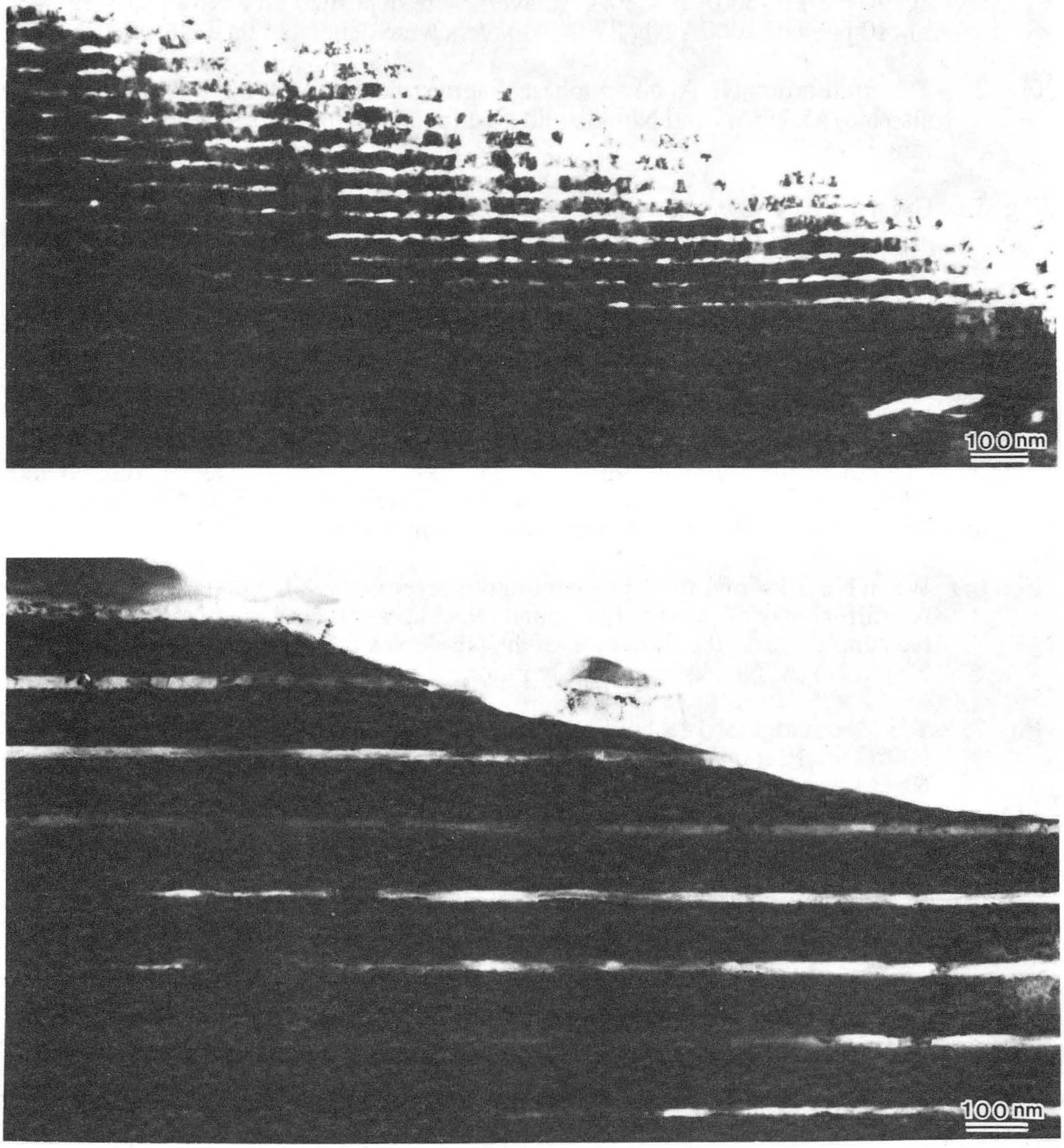

XBB 872-1281

Figure 1

Nb-Al Phase diagram

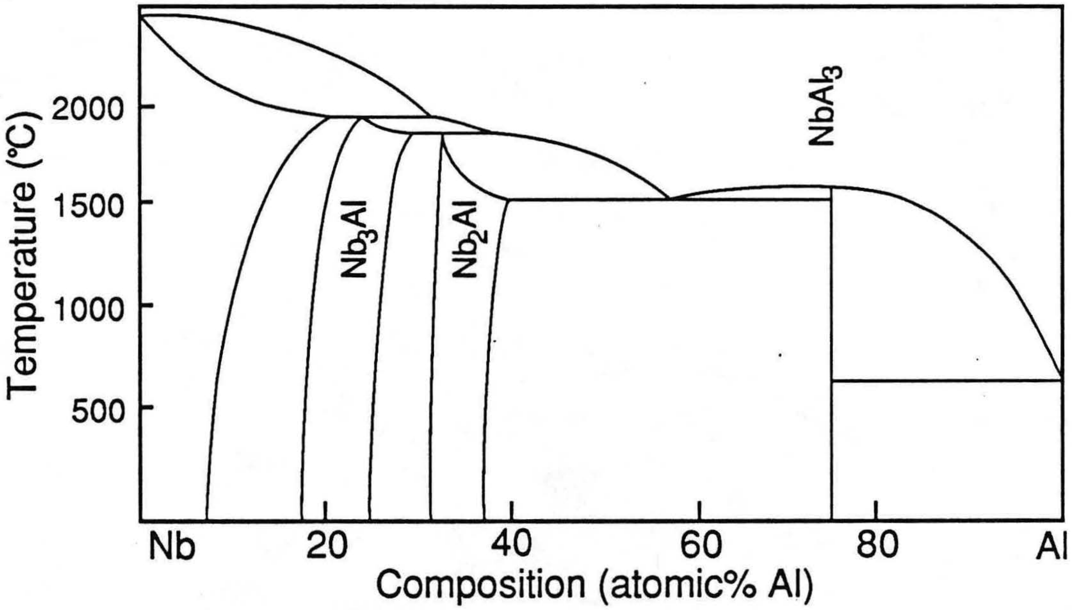

Figure 2

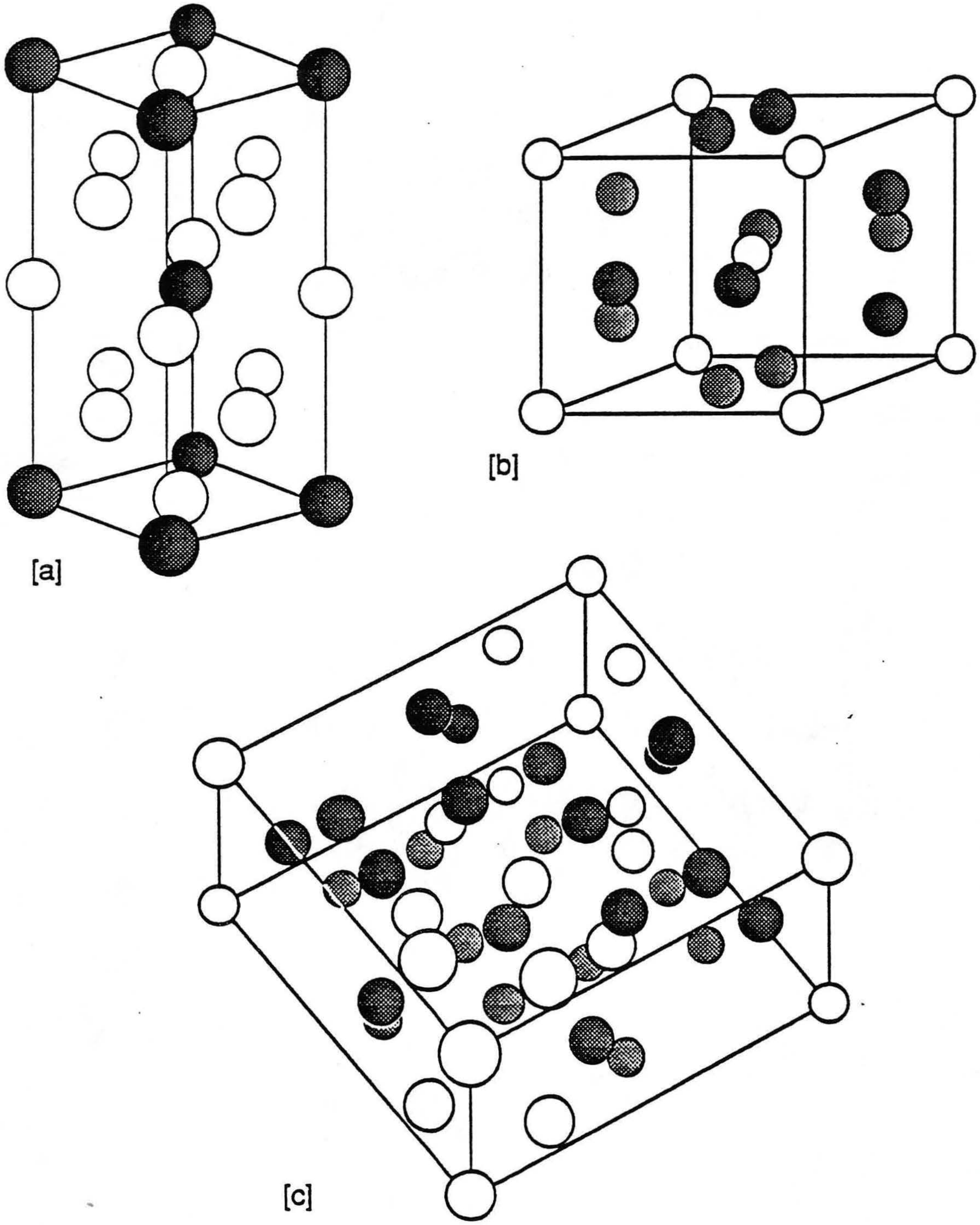

Figure 3

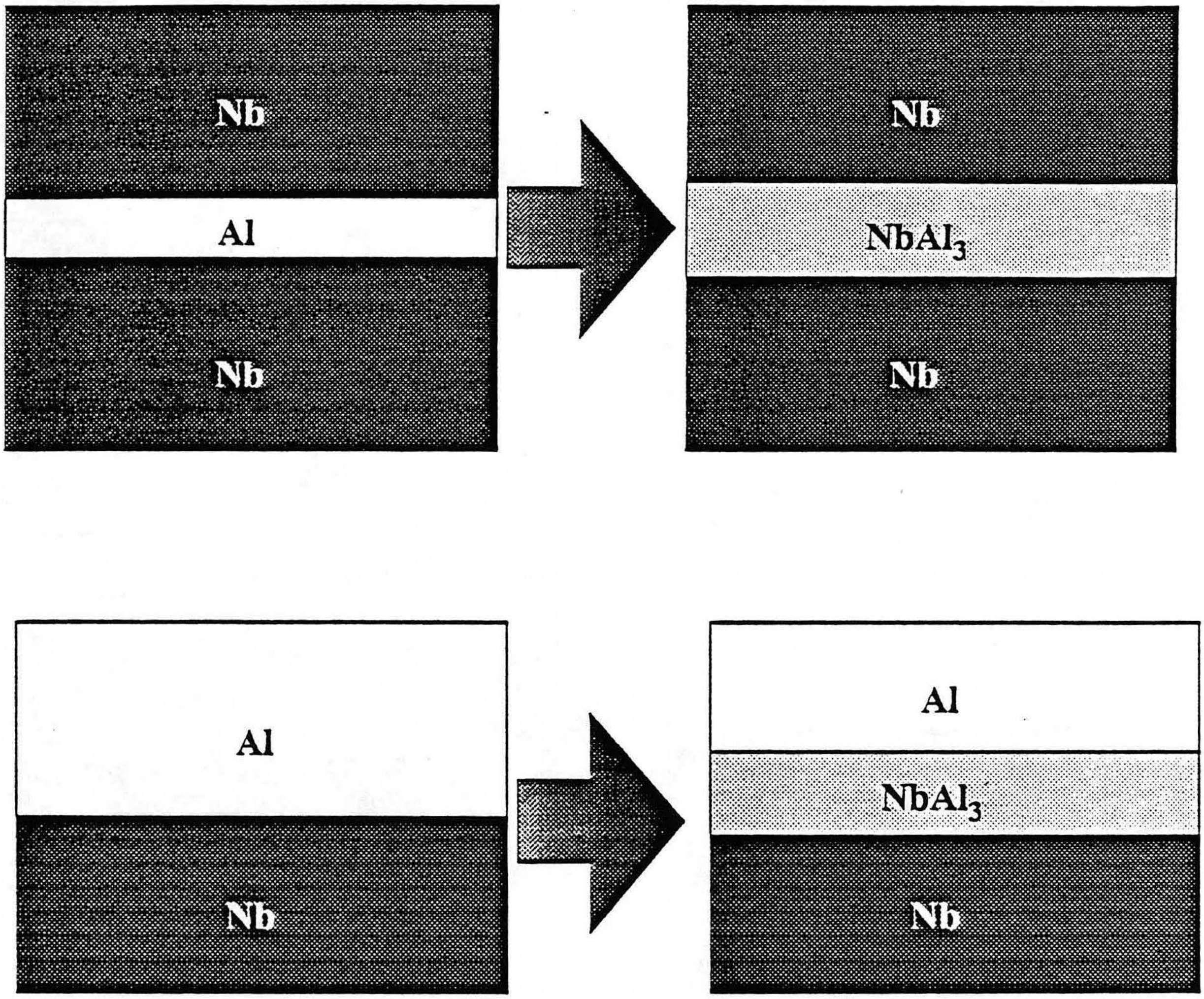

Figure 4

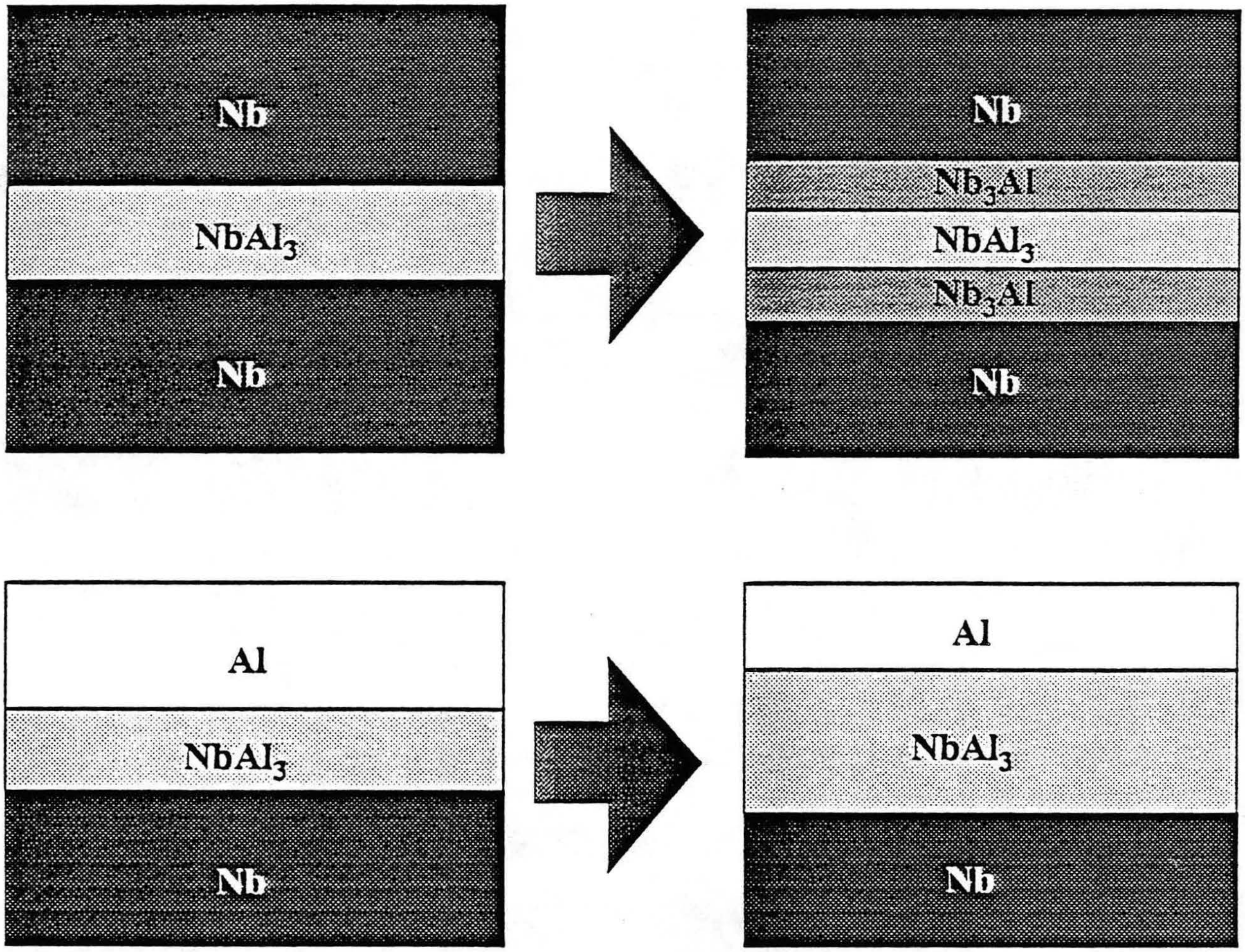

Figure 5

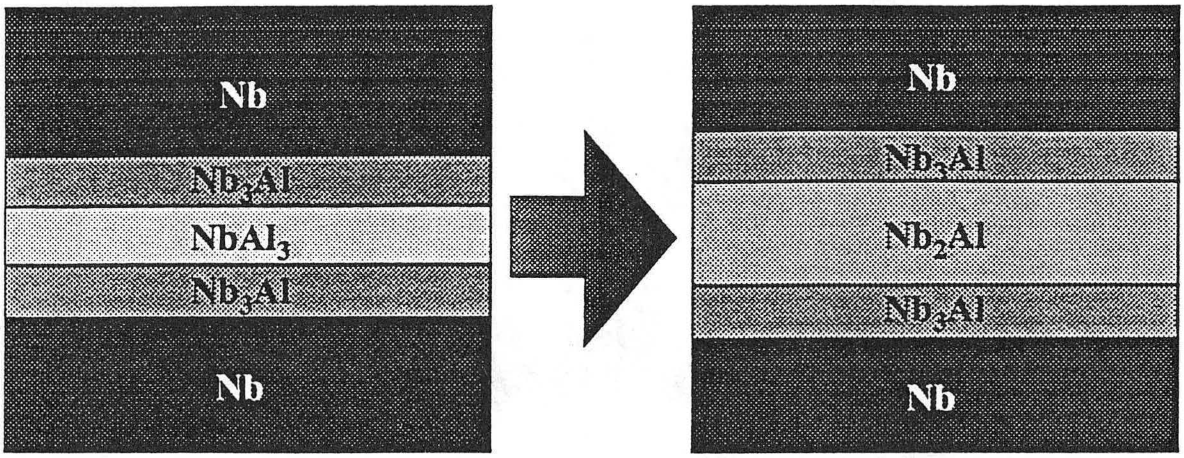

Figure 6

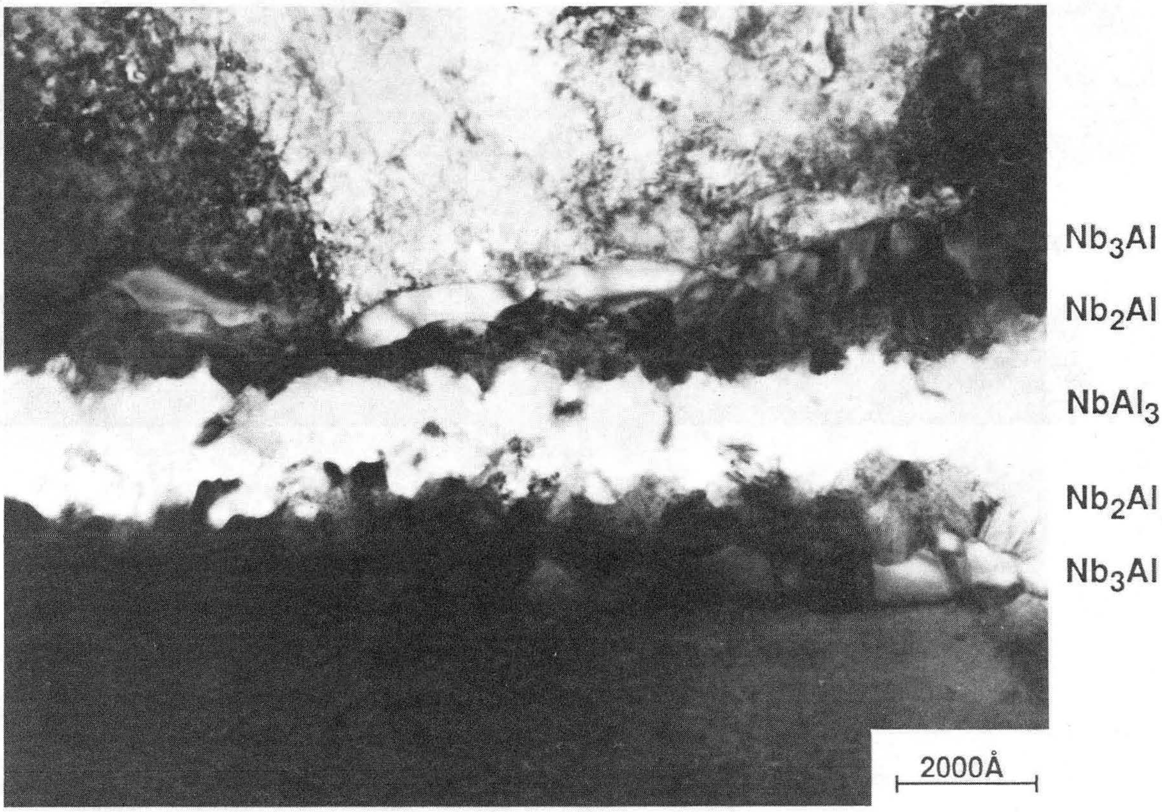

XBB 884-2851

Figure 7

	< 650°C	> 700°C	Al layer thickness
Nb + Al	$NbAl_3$	$NbAl_3$	>> 1µm
Nb + Al	$NbAl_3$ (+ Nb)	Nb_3Al	≤ 300Å
Nb + Al	$NbAl_3$ (+ Nb)	Nb_3Al+Nb_2Al*	intermediate

LAWRENCE BERKELEY LABORATORY
TECHNICAL INFORMATION DEPARTMENT
UNIVERSITY OF CALIFORNIA
BERKELEY, CALIFORNIA 94720